Effects of temperature and point defects on the stability of C15 Laves phase in iron: A molecular dynamics investigation*

Hao Wang(王昊)[1,2], Ning Gao(高宁)[3,†], Guang-Hong Lü(吕广宏)[1], and Zhong-Wen Yao(姚仲文)[2,‡]

[1] School of Physics and Nuclear Energy Engineering, Beihang University, Beijing 100190, China
[2] Mechanical and Materials Engineering, Queen's University, Kinston, ON K7L 3N6, Canada
[3] Institute of Modern Physics, Chinese Academy of Sciences, Lanzhou 730000, China

(Received 13 September 2017; revised manuscript received 8 February 2018; published online 10 May 2018)

Molecular dynamics simulations are used to investigate the stabilities of C15 Laves phase structures subjected to temperature and point defects. The simulations based on different empirical potentials show that the bulk perfect C15 Laves phase appears to be stable under a critical temperature in a range from 350 K to 450 K, beyond which it becomes disordered and experiences an abrupt decrement of elastic modulus. In the presence of both vacancy and self-interstitial, the bulk C15 Laves phase becomes unstable at room temperature and prefers to transform into an imperfect body centered cubic (BCC) structure containing free vacancies or vacancy clusters. When a C15 cluster is embedded in BCC iron, the annihilation of interstitials occurs due to the presence of the vacancy, while it exhibits a phase transformation into a $(1/2)\langle 111\rangle$ dislocation loop due to the presence of the self-interstitial.

Keywords: C15 Laves phase, stability, elastic modulus, structural evolution

PACS: 61.80.–x, 61.80.Az, 61.82.Bg, 31.15.xv **DOI:** 10.1088/1674-1056/27/6/066104

1. Introduction

The formation of point defects, e.g., a vacancy and self-interstitial atom (SIA), induced by neutron irradiations in nuclear materials, has been known about for decades. To understand their properties (e.g., the stable state, clustering, and evolution) is a key to studying the radiation damages. For example, the $\langle 110\rangle$ dumbbell in body centered cubic (BCC) iron has been confirmed to be the most stable SIA configuration by the density functional theory (DFT) calculation and experimental measurement,[1,2] while for other BCC transition metals (e.g., tungsten), the $\langle 111\rangle$ crowdion is the most stable self-interstitial state.[3] Because of the high binding energy between SIAs, the SIA-clusters can also form in the atomic displacement cascade and/or the following evolution process of defects. The primary configuration of the SIA-cluster is the dislocation loop, which has been observed with transmission electron microscopy (TEM)[4] and also predicted theoretically by molecular dynamics (MD) calculations.[5,6] The Burgers vector of these loops in BCC iron is either $(1/2)\langle 111\rangle$or $\langle 100\rangle$.[6–8] The number ratio between these two loops depends on the irradiation temperature, ion flux, etc.[9] For $(1/2)\langle 111\rangle$ loops, MD calculations show that such a loop has lower migration energy and may be absorbed at grain boundaries.[10–12] For the $\langle 100\rangle$ loop, its formation mechanism is one of the recent hot topics and different theories have been suggested accordingly.[11,13,14] Except the dislocation loop, the Bacon group also reported a three-dimensional (3D) metastable sessile di-interstitials structure that has 12 interstitials placed at the edges of a truncated tetrahedron, sharing 10 lattice sites in the irradiated BCC iron, which leads to only two additional atoms in the BCC lattice.[15,16] Such a structure corresponds to the C15 Laves phase.[17] The DFT calculations show that the self-interstitial cluster with C15 Laves phase structure in BCC iron has lower formation energy, higher stability and immobility than the other known SIA-cluster configurations, and can grow by capturing single SIAs.[17] When the number of SIAs is limited, DFT results demonstrate that the tetra- and octa-interstitial clusters with C15 structure have the lowest energy state in all known SIA-cluster configurations in BCC iron.[18,19] MD results showed that C15 clusters can transform into $\langle 100\rangle$ and $(1/2)\langle 111\rangle$ loops with a size of 20–30 interstitials.[19] Although the theoretical calculation predicts that C15 clusters form under irradiation, they are rarely observed experimentally.[15–18] Except the susceptibility of the experimental observational technique, there are several factors in the above experimental results: temperature, damage rate, and the effect of point defects, which may affect the lifetime of the C15 phase. In order to provide the possible understanding of the above puzzles, MD simulation is used in this work to explore the stability of the C15 Laves phase, especially to investigate the kinetic properties of the C15 phase at different temperatures. The following factors are mainly studied

*Project supported by the National Natural Science Foundation of China (Grant Nos. 11675230 and 11375242) and Canada's Natural Sciences and Engineering Research Council NSERC Discovery Grant and Canada Foundation for Innovation CFI.

†Corresponding author. E-mail: ning.gao@impcas.ac.cn
‡Corresponding author. E-mail: yaoz@queensu.ca

© 2018 Chinese Physical Society and IOP Publishing Ltd

through MD simulations: 1) the temperature-dependent elastic modulus and structure evolution of perfect C15 Laves iron lattice; 2) structural evolution of C15 Laves iron lattice under the effect of single point defect (SIA or vacancy) at different temperatures, furthermore, for C15 Laves phase cluster embedded in BCC iron; 3) the possible transform driven by point defects and the related critical phase transformation temperature have also been studied. In Section 2, the method is briefly described. The results are presented and discussed in Section 3, and conclusions are drawn in Section 4, finally.

2. Method

The A04[20] and M07[13,17] empirical potentials are mainly employed in the present simulations. These potentials are commonly used for studying the radiation damages and have been used in previous studies of the C15 Laves phase.[13,17–19] These previous studies showed that the A04 potential considerably underestimates the stabilities of C15 clusters and the M07 potential slightly overestimates their stabilities in comparison with DFT data.[17] A cubic box with 4×4×4 unit cells and periodic boundary conditions are used in this work. The size effect is also examined using a larger simulation box (20×20×20), which shows the same results as those obtained with the small box. The system is relaxed first via molecular statics (MS) simulation, and then MD calculations are carried out with a time-step of 1 fs. Common neighbor analysis (CNA) in OVITO[21] is mainly used to analyze the structural evolution with the temperature dependence and to identify the defects in the BCC and C15 matrix.

After the complete MS relaxations, the formation energy E^{f} of a single defect is calculated from the following equation:

$$E_{\mathrm{f}} = E^{\mathrm{def}} - E^{\mathrm{perf}} \cdot \frac{N^{\mathrm{def}}}{N^{\mathrm{perf}}}, \tag{1}$$

where N^{def} and E^{def} are the number of atoms and total energy of the system including the defects, E^{perf} is the energy of the perfect lattice, and N^{perf} is the number of atoms in a perfect lattice.

To study the temperature-dependent structural evolution, the MS and MD simulations are performed alternatively. The structure evolution is visualized using OVITO.[21] After MS relaxation, the system is relaxed with an isothermal–isobaric (NPT) ensemble at each temperature for 100 ps to approach to thermal equilibrium. Further relaxation is performed for 20 ps with a canonical (NVT) ensemble, in which the last 2-ps relaxation results are used for the calculation of the temperature-dependent elastic constants C_{ijkl} following the method developed by Ray *et al.*[22–24]

$$\begin{aligned} C_{ijkl} = & -\frac{v_0}{k_{\mathrm{B}}T}\left(\langle P_{ij}P_{kl}\rangle - \langle P_{ij}\rangle\langle P_{kl}\rangle\right) \\ & + \frac{2Nk_{\mathrm{B}}T}{v_0}\left(\delta_{ik}\delta_{jl} + \delta_{il}\delta_{jk}\right) \\ & + \langle B1_{ijkl}\rangle + \langle B2_{ijkl}\rangle + \langle B3_{ijkl}\rangle, \end{aligned} \tag{2}$$

where T is the temperature of the system, k_{B} is the Boltzmann constant, P_{ij} is the microscopic stress tensor of σ calculated by the Parrinello–Rahman method,[23] which includes the contributions from momentum and force of N particles in volume V_0, δ_{ik} is Kronecker delta, and $B1_{ijkl}$, $B2_{ijkl}$, and $B3_{ijkl}$ are three Born terms[23]

$$B1_{ijkl} = \frac{1}{v_0}\sum_{\substack{a,b=1\\a<b}}\left(\phi''_{ab} - \frac{\phi'_{ab}}{r_{ab}}\right)\frac{x_{abi}x_{abj}x_{abk}x_{abl}}{r^2_{ab}}, \tag{3}$$

$$B2_{ijkl} = \frac{1}{v_0}\sum_{\substack{a,b=1\\a<b}}F'_a\left(\rho^{at''}_b - \frac{\rho^{at'}_b}{r_{ab}}\right)\frac{x_{abi}x_{abj}x_{abk}x_{abl}}{r^2_{ab}}, \tag{4}$$

$$B3_{ijkl} = \frac{1}{v_0}\sum_{a,b=1}^{N}F''_a g_{aij}g_{akl}, \tag{5}$$

$$g_{aij} = \sum_{\substack{b=1\\b\neq a}}\frac{\rho^{at'}_b x_{abi}x_{abj}}{r_{ab}}, \tag{6}$$

where F_a is the force on atom a, ϕ_{ab} is the interatomic potential evaluated at the interatomic distance r_{ab} between atoms a and b, x_{abi} is the i-th component of the relative position vector of atoms a and b, and ρ^{at} is the atomic (at) electron density.

It should be noted that the elastic constants calculated from Eq. (2) are 4-th order tensor for a BCC lattice at a given temperature, that is, the calculated elastic constants are then isothermal properties. There are three independent values: $C_{11} = C_{1111}$, $C_{12} = C_{1122}$, and $C_{44} = C_{2323}$. The shear and Young's modulus defined as $G = C_{44}$, and $E = C_{44}(3C_{11} - 4C_{44})/(C_{11} - C_{44})$ are then calculated accordingly.

3. Results and discussion

3.1. Perfect C15 Laves phase

For a perfect C15 Laves phase, its mechanical stability was investigated by analyzing the shear and Young's moduli versus temperature. The configuration of a unit cell of the C15 Laves phase is provided in Fig. S1 in the supplementary materials. In this work, these two moduli are calculated in a temperature range from 0 K to 450 K in steps of 25 K. The obtained results are shown in Fig. 1. The example of error bars is shown in the inserted image in the figure. From Eq. (2), it is clear that the method based on thermal fluctuation is the main reason for resulting in the small error bars in this work. Compared with the results of BCC iron,[25] C15 shows anomalous elastic properties calculated by the A04 potential at temperatures lower than 400 K, that is, the moduli increase slightly with the temperature increasing from 0 K to 425 K, and then rapidly decrease when the

temperature is higher than 425 K. The elastic moduli calculated by the M07 potential indicate similar anomalous elastic properties at the temperatures lower than 350 K. However, a local minimal Young's modulus is obtained in a temperature range from 0 K to 25 K, which is considered to be mainly related to the contributions from the second derivative of potentials. The details of the above analysis are provided in the supplementary materials. When the temperature is higher than 375 K, the rapid decreasing of elastic properties also occurs. Although the dependence of the modulus on the temperature of the C15 Laves phase is different from the cases in normal metals,[25] a similar tendency has also been observed in other materials such as $Hf_{25}V_{60}Nb_{15}$ and TaV_2,[26,27] which are of the C15 Laves phase structure. Based on these previous studies, the mechanism of the anomalous elastic properties on C15 materials may be attributed to the electronic band-structure effect on the elastic constant C_{44} of the system.[28,29] In Fig. 1, the detailed analysis indicates that rapid decreases of moduli are mainly related to the phase transformation from the initial C15 phase to a disordered phase. In order to investigate such a phase transformation, the atom rearrangement processes of the perfect C15 Laves phase under different temperatures are then carefully followed. The examples projected on the basal (XY) plane calculated by the A04 potential[20] are shown in Fig. 2. It is found that the C15 Laves phase calculated by the A04 potential is stable when the temperature is lower than 400 K. With the M07 potential,[13,17] the C15 Laves phase is stable when the temperature is lower than 350 K. When the temperature reaches up to 400 K or 350 K, thermal fluctuation results in the atomic disorder in a small region of the system (Fig. 2(b)). With the increase of the temperature from 400 K to 425 K calculated by the A04 potential and 350 K to 375 K calculated by the M07 potential, more atoms are in disordered states. When the temperature is around 450 K and 375 K predicted by two potentials, respectively, the system loses stability, reaching a full disordered state as shown in Figs. 2(b)–2(d). Although the exact transformation temperature of the perfect C15 Laves phase predicted by the MD method depends on the interatomic potential used in the simulation, the loss of stability behavior can be certainly characterized in a certain temperature range, that is, from 350 K to 450 K by these two potentials. Thus, the effect of temperature is one of the reasons for inducing the disorder of the C15 Laves phase. Taking into account the modulus variation and the atomic rearrangement process with temperature, it is concluded that the bulk perfect C15 Laves phase will lose its stability with increasing temperature.

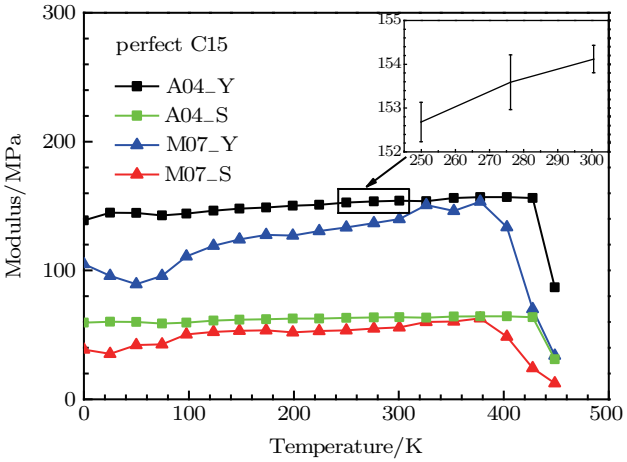


Fig. 1. (color online) Young's and shear moduli of a perfect C15 Laves phase structure at different temperatures, calculated by A04[20] and M07[13,17] potentials. The enlarged drawing shows the local error bars of temperature-dependent modulus.

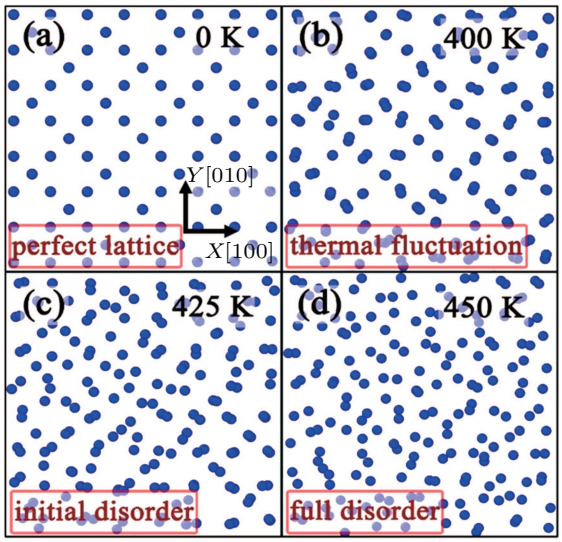


Fig. 2. (color online) Snapshots of the evolution of C15 Laves phase calculated by A04 potential[20] from the perfect structure to disordered state. (a) Initial structure relaxed at 0 K; [(b)–(d)] transient states at 400 K, 425 K, and 450 K respectively after MD relaxations.

3.2. C15 Laves phase with point defects

Except the effect of temperature on the stability of the perfect C15 Laves phase, the effect of point defects should also be studied because the formation of these defects is inevitable under irradiation in reactors. Based on the calculations of atomic potential energy states, the atoms in the C15 Lave phase are divided into two different atomic sites, thus, resulting in different states of vacancy and SIAs. Type-A atoms located at diamond cubic sites with energy around −4.253 eV by using the A04 potential, and those around −4.534 eV by using the M07 potential are investigated separately. Type-B atoms located at tetrahedral sites with energy around −3.623 eV by using the A04 potential and those around −3.584 eV by using the M07 potential are studied. Thus, the type-A atoms are much more stable than the type-B atoms. By removing a type-A or type-B atom, a single vacancy referred to as A-vac or

B-vac is created. By inserting an interstitial around a type-A or type-B atom, a ⟨100⟩, ⟨110⟩ or ⟨111⟩ dumbbell/crowdion is built along one of three coordinate axis directions. It should be noted that configurations of the above dumbbell and crowdion are created just based on previous studies in BCC iron.[1–3] The relaxation may result in different interstitial structures as explained in the following.

The calculation results show that the formation of both type-A and type-B vacancies in a perfect C15 Laves phase can result in the instability of the system. The phase transformation temperatures of C15 calculated by the A04 potential with a type-A vacancy and a type-B vacancy are 260 K and 200 K, respectively. The phase transformation temperatures of C15 calculated by the M07 potential with a type-A vacancy and a type-B vacancy are 290 K and 110 K, respectively. Compared with the results from the phase transformation of the perfect C15 phase as discussed in Subsection 3.1, these results imply that the appearance of a vacancy decreases the critical temperature of the phase transformation from a perfect lattice to a disordered state. When the interstitial defect appears in the C15 phase, the results calculated by the A04 potential show that after relaxation, the initial ⟨100⟩, ⟨110⟩ or ⟨111⟩ dumbbell or crowdion interstitial would first result in the symmetrical movements of the nearby atoms on the same atomic plane of the interstitial to form a symmetrical defect structure as shown in Fig. 3.

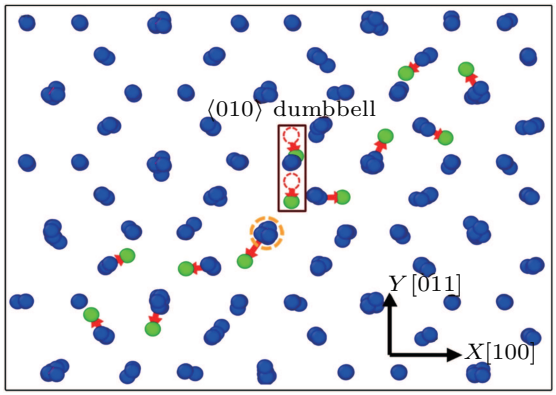


Fig. 3. (color online) Interstitial structure in C15 Laves phase formed after MS relaxation from the initial ⟨010⟩ dumbbell, calculated with A04 potential.[20] The two red dash circles indicate the positions of the original ⟨010⟩ dumbbell. The red arrow shows the displacement vector of atom from the original (blue spheres) to the final (green spheres) states.

It is found that all the initial dumbbells or crowdions studied in this work can result in the above structure. The M07 potential is adopted, resulting in a similar state but without showing symmetrical properties. The formation of this structure is also indicated by the displacement vectors of atoms as shown in the figure, where one atom of the dumbbell moves back to the mass center of the dumbbell, forcing another atom of the dumbbell to move away from its original position, leading to a series of atom displacements and the formation of such a symmetrical defect structure (Fig. 3). Based on the above results, the effects of an interstitial on the stability of the C15 Laves phase are further studied by performing MD simulations at different temperatures. The critical temperature for the system transforming from the perfect to disordered state under the effect of one interstitial is around 100 K predicted by two different potentials, lower than in the case of a perfect lattice or containing a single vacancy. Furthermore, if both the interstitial and vacancy exist together in the C15 Laves phase, a similar disordered process is also observed with even lower critical temperature (∼ 80 K). Hence, both interstitial and vacancy can result in the instability of the C15 Laves phase with lower critical transformation temperatures. It should also be noted that when the density of defects increases, the lower phase transition temperature is observed.

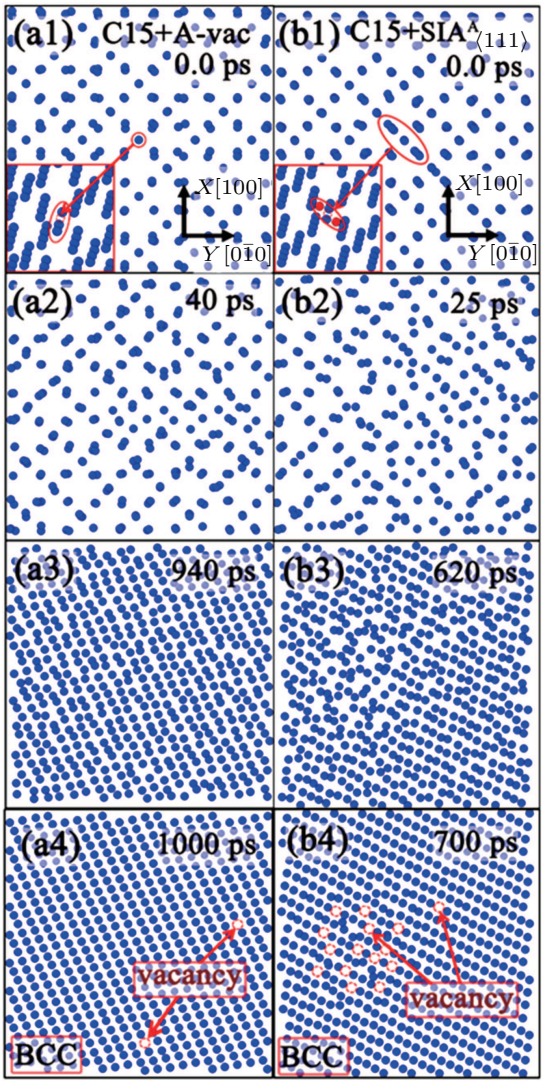


Fig. 4. (color online) Phase transformations of C15 Laves phase containing (a) a vacancy and (b) an SIA, calculated with the A04 potential.[20] Atomic projections are on the basal (*XY*) plane. [(a1) and (b1)] Initial states after relaxation at time zero. [(a2)–(a4)] and [(b2)–(b4)] Structural evolutions at 300 K, (a4) and (b4) final BCC lattice structures containing vacancies or vacancy clusters.

After the phase transformation from C15 to the disordered

state due to the temperature change or the appearance of defects, long time MD simulations also indicate that the further phase transformation from the disordered state to a BCC lattice state can also occur. The structure evolution process of C15 with a type-A vacancy or a type-A ⟨010⟩ dumbbell at 300 K simulated by A04 and M07 potential are similar as shown by the examples in Fig. 4, which are obtained with A04 potential. The initial states are the configurations at 0 femtosecond but after full MS relaxations (Figs. 4(a1) and 4(b1)). The snapshots of the structures at different times show that in the system of C15 containing a single point defect, thermal fluctuation drives the atoms to move to their new equilibrium positions at the times around 940 ps and 620 ps (Figs. 4(a2) and 4(a3), and Figs. 4(b2) and 4(b3)). After the further relaxation, it can be found that the formed lattice is an imperfect BCC structure containing vacancies and vacancy clusters as analyzed by the CNA method (Figs. 4(a4) and 4(b4)). Since the atomic density of BCC iron is around 0.0859/Å^3, higher than that of C15 Laves phase (0.0820/Å^3), thus, vacancies or vacancy clusters are expected to form during the transformation from C15 Laves phase to BCC lattice structure as indicated by Figs. 4(a4) and 4(b4).

3.3. C15 Laves phase cluster embedded in BCC iron

In the present work, in order to understand the temperature-dependent stability of the C15 Laves phase cluster embedded in the BCC iron, the BCC iron simulation box with 30×30×30 unit cells containing a C15 cluster with two interstitials up to tens of interstitials is built for MD simulations at different temperatures. The C15 clusters can spontaneously transform into an SIA-cluster composed of the parallel ⟨111⟩ crowdions or loops, depending on the critical temperatures and the size of the C15 clusters (see Table 1). It is clear that the range of phase transformation temperature of 28 interstitial C15 clusters calculated by the M07 potential is from 1135 K to 1800 K. However, when the number of interstitials in the C15 cluster is more than 10, the phase transformation temperature predicted by this potential is higher than 1800 K, which is not listed in the table. The range of phase transformation temperature calculated by the A04 potential is from 845 K to 1535 K for a C15 defect containing 210 interstitials. Thus, although there is a time limitation of the MD method, the higher temperature is required for the phase transformation of a larger C15 cluster.

Table 1. The phase transformation temperature of a C15 cluster containing di-interstitial to deca-interstitial.

	I_2^{C15}	I_3^{C15}	I_4^{C15}	I_5^{C15}	I_6^{C15}	I_7^{C15}	I_8^{C15}	I_9^{C15}	I_{10}^{C15}
T_{M07}/K	1165	1135	1485	1550	1690	1715	1775	1785	1800
T_{A04}/K	875	845	1250	1310	1400	1465	1500	1520	1535

Considering the radiation environment, the influences of the additional vacancy and interstitial on the stability of the C15 Laves phase in BCC iron are also studied. As an example, the I_4^{C15} defect is considered since it is regarded as the smallest stable C15 unit and also the more stable C15 structure than the other 4-interstitial configurations (such as parallel ⟨111⟩ crowdion configurations or loops).[18] The radius of an I_4^{C15} cluster is around 3.51 Å. The defects (vacancy or ⟨110⟩ dumbbell) are inserted near the I_4^{C15} cluster within the distance around 1 to 2 lattice constants of iron. Considering the size of the C15 Laves phase, the number of these defects is set to be from 1 to 8. The results calculated with A04 and M07 potentials show that at 300 K, the existence of vacancies will first annihilate the interstitial of the C15 Laves phase and then convert the structural transformation of the I_4^{C15} cluster into a complete BCC Fe phase. The examples of the structure evolution of an I_4^{C15} with seven vacancies around it at 300 K calculated with the A04 potential are given in Fig. 5 in the time sequence. From Figs. 5(a1)–5(a4), it is clearly seen that the nearby vacancies are easy to recombine with SIAs from the I_4^{C15} cluster, resulting in the transformation from the C15 Laves phase to the BCC iron phase. Because of the different atomic densities, the final state of the system is again the BCC iron lattice mixed with separated vacancies or vacancy cluster. Regarding the effect of interstitials on the possible phase transformation of an I_4^{C15} defect in BCC iron, the results calculated with the A04 potential show that the I_4^{C15} cluster transforms into a loop with a Burgers vector of (1/2)⟨111⟩ even at 300 K as shown in Figs. 5(b1)–5(b4). The interaction between the I_4^{C15} cluster and the ⟨110⟩ dumbbells induces the interstitial atoms in the C15 Laves phase to rearrange into the ⟨111⟩ crowdions and then to transform these atoms into a (1/2)⟨111⟩ interstitial loop. However, the results calculated with the M07 potential show the growth of the C15 cluster after absorbing the incoming interstitials at 300 K, which is similar to the results reported by Zhang *et al.*[19] When the C15 cluster contains more than 2030 interstitials, its transformation into ⟨100⟩ or (1/2)⟨111⟩ loops is also observed.[19] The results predicated by the M07 potential indicate that when the number of absorbed free interstitials is less than that of the interstitials of the C15 cluster, the structure of the C15 cluster is difficult to change before the temperature rises up to more than 1800 K. However, the C15 clusters will spontaneously transform into loops at the temperature lower than 1250 K when the number of added interstitials is more than that of the interstitials of the C15 cluster. Thus, the above results imply that the A04

potential predicts a much lower critical temperature than the M07 potential for a C15 phase to transform into loops. When the size of the embedded C15 Laves phase increases, a similar transformation driven by an additional vacancy or interstitial is also observed.

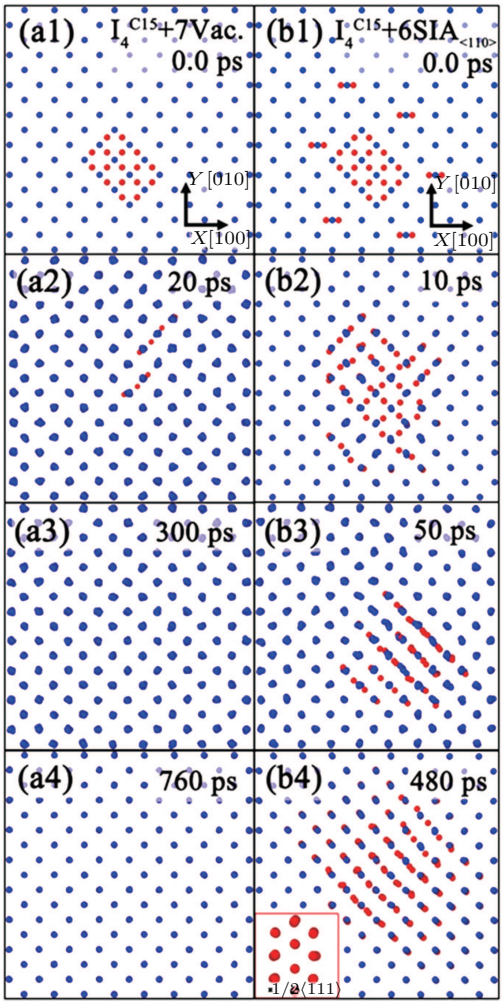


Fig. 5. (color online) Phase transformation processes at 300 K for an I_4^{C15}cluster embedded in BCC iron with (a) seven randomly placed nearby vacancies and (b) six randomly placed nearby ⟨110⟩ dumbbells. The atomic projection is in the basal (XY) plane. [(a1) and (b1)] Initial structures; [(a2) and (b2)] structures after relaxation at 0 K; [(a3) and (b3)] states after relaxation at 300 K; [(a4) and (b4)] final structures after full phase transformation. Blue and red spheres indicate iron base atoms and interstitials, respectively. Inserted image in panel (b4) shows the loop structure viewed along the Burgers vector ((1/2)⟨111⟩) direction. The illustrations are obtained with A04 potential.[20]

4. Conclusions

The effects of point defects and temperature on the stability of the C15 Laves phase structure of Fe have been investigated via the molecular dynamic simulations. A bulk perfect C15 Laves phase is stable at room temperature, and it exhibits a phase transformation into a BCC lattice structure with increasing temperature in a range of 350 K–450 K, depending on the employed interatomic potentials. The presence of a single point defect reduces the temperature of such a phase transformation. For a C15 cluster embedded in Fe, the spontaneous transformations occur at the critical C15 size with around 2–8 interstitials. The presence of both vacancy and interstitial in the vicinity of a C15 cluster can result in its phase transformation through either the annihilation of interstitials in the C15 phase or the formation of a (1/2)⟨111⟩ dislocation loop, depending on the critical temperature and the number of added point defects. Therefore, considering the harsh environment (e.g., high temperatures, supersaturated interstitials and vacancies) in nuclear reactors, the C15 Laves phase may exist in a visible period during irradiation, but it has rarely been observed with transmission electron microscopy measurement.

Appendix A: Supplementary materials

The configuration of a unit cell of the C15 Laves phase is shown below.

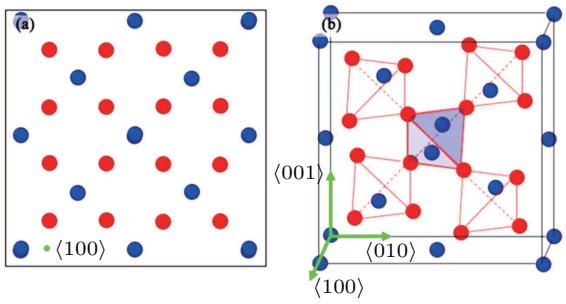


Fig. S1. (color online) Bulk C15 Laves phase in a unit cell. (a) Atomic projection in the basal plane (XY) and (b) 3D configuration from the ⟨100⟩ direction. Blue atoms are the type-A atoms located at diamond cubic sites, and red atoms are the type-B atoms located at tetrahedral sites.

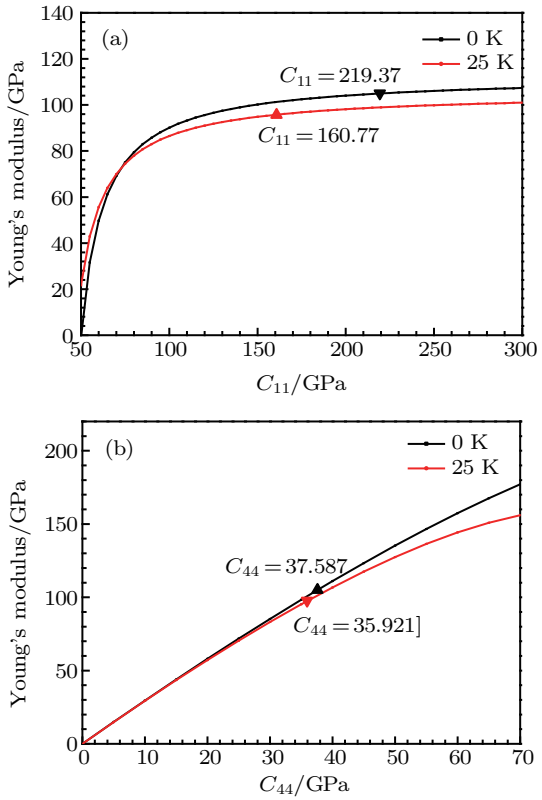


Fig. S2. (color online) Plots of Young's modulus versus elastic constant (a) C_{11} and (b) C_{44} at temperatures of 0 K and 25 K.

In Fig. 1, the calculations with the M07[13,17] potential show that both Young's moduli decrease with temperature increasing from 0 K to 25 K and a local minimal value is also observed at lower temperatures. Since Young's modulus is mainly related to C_{11} and C_{44}, the dependence of Young's modulus on these two elastic constants from 0 K and 25 K is expressed as $E = C_{44}(3C_{11} - 4C_{44})/(C_{11} - C_{44})$ and shown in Fig. S2 (e.g. the values of C_{44} at 0 K and 25 K should be substituted into this equation to plot the curve of C_{11}). From these two figures, it is clearly seen that the decrease of Young's modulus is induced mainly by the decrease of C_{11}.

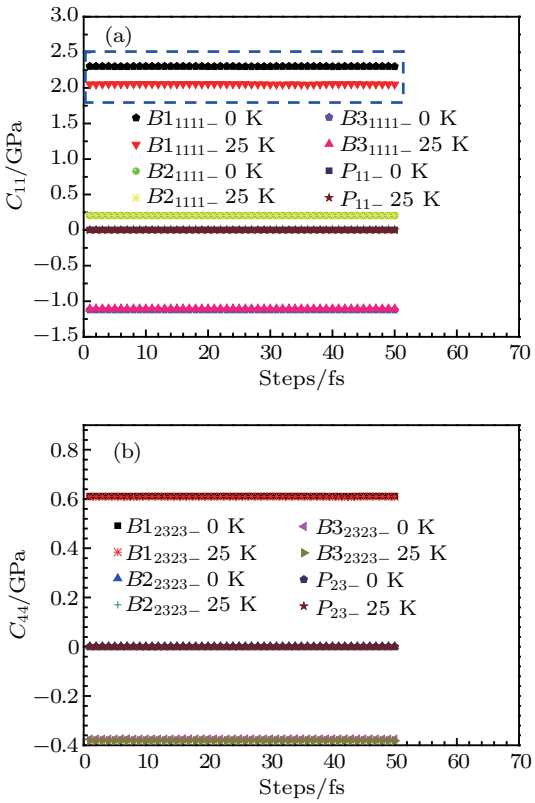


Fig. S3. (color online) $B1_{ijkl}$, $B2_{ijkl}$, $B3_{ijkl}$, and P_{ij} of (elastic constants (a) C_{11} and (b) C_{44} at 0 K and 25 K.

Since the temperature increase is limited in a range from 0 K to 25 K, the decrease of C_{11} is mainly from the decrease of $B1_{1111}$, $B2_{1111}$, $B3_{1111}$, or P_{11} (from Eq. (2). From Fig. S3, the $B1_{1111}$ is found to be the main reason for inducing the decrease of C_{11}. In Eq. (2), the $B1_{1111}$ is related to the second derivative of potential, thus, the intrinsic properties of the second derivative of potential is considered as the main reason for inducing the decrease of Young's moduli at lower temperatures.

References

[1] Domain C and Becquart C 2001 *Phys. Rev. B* **65** 024103
[2] Fu C C, Willaime F and Ordejón P 2004 *Phys. Rev. Lett.* **92** 175503
[3] Nguyen-Manh D, Horsfield A P and Dudarev S L 2006 *Phys. Rev. B* **73** 020101
[4] Arakawa K, Ono K, Isshiki M, Mimura K, Uchikoshi M and Mori H 2007 *Science* **318** 956
[5] Wirth B D, Odette G R, Maroudas D and Lucas G E 2000 *J. Nucl. Mater.* **276** 33
[6] Dudarev S L, Bullough R and Derlet P M 2008 *Phys. Rev. Lett.* **100** 135503
[7] Masters B C 1965 *Philos. Mag.* **11** 881
[8] Eyre B L and Bullough R 1965 *Philos. Mag.* **12** 31
[9] Yao Z, Jenkins M L, Hernández-Mayoral M and Kirk M 2010 *Philos. Mag.* **90** 4623
[10] Osetsky Y N, Bacon D J, Serra A, Singh B N and Golubov S I 2000 *J. Nucl. Mater.* **276** 65
[11] Marian J, Wirth B D and Perlado J M 2002 *Phys. Rev. Lett.* **88** 255507
[12] Dérès J, Proville L and Marinica M 2015 *Acta Mater.* **99** 99
[13] Malerba L, Marinica M C, Anento N, Bjorkas C, Nguyen H, Domain C, Djurabekova F, Olsson P, Nordlund K, Serra A, Terentyev D, Willaime F and Becquart C S 2010 *J. Nucl. Mater.* **406** 19
[14] Gao N, Chen J, Kurtz RJ, Wang ZG, Zhang R F and Gao F 2017 *J. Phys.: Condens. Matter* **29** 455301
[15] Gao F, Bacon D J, Osetsky Y N, Flewitt P E J and Lewis T A 2000 *J. Nucl. Mater.* **276** 213
[16] Bacon D J, Gao F and Osetsky Y N 2000 *J. Nucl. Mater.* **276** 1
[17] Marinica M C, Willaime F and Crocombette J P 2012 *Phys. Rev. Lett.* **108** 025501
[18] Dézerald L, Marinica M C, Ventelon L, Rodney D and Willaime F 2014 *J. Nucl. Mater.* **449** 219
[19] Zhang Y, Bai X M, Tonks M R and Biner S B 2015 *Scr. Mater.* **98** 5
[20] Ackland G J, Mendelev M I, Srolovitz D J, Han S and Barashev A V 2004 *J. Phys.: Condens. Matter* **16** S2629
[21] Alexander K C, Schuh C A, Panzarino J F, Ramos J J and Rupert T J 2010 *Modelling Simul. Mater. Sci. Eng.* **18** 015012
[22] Ray J R, Moody M C and Rahman A 1985 *Phys. Rev. B* **32** 733
[23] Wolf J, Mansour K A, Lee M W and Ray J R 1992 *Phys. Rev. B* **46** 8027
[24] Ray J R and Rahman A 1984 *J. Chem. Phys.* **82** 4243
[25] Adams J J, Agosta D S, Leisure R G and Ledbetter H 2006 *J. Appl. Phys.* **100** 113530
[26] Chu F, Lei M, Migliori A, Chen S P and Mitchell T E 1994 *Philos. Mag. B* **70** 867
[27] Foster K, Hightower J E, Leisuret R G and Skripov A V 2000 *Philos. Mag. B* **80** 1667
[28] Izyumov, Yu. A, Naysh, and Ye V N, V. and Syromyatnikov 1975 *Fiz. Metal. Metalloved.* **39** 455
[29] Chu F, Šob M, Siegl R, Mitchell T E and Chen S P 1994 *Philos. Mag. B* **70** 881